European Journal of Radiology 118 (2019) 169–174

Contents lists available at ScienceDirect

European Journal of Radiology

journal homepage: www.elsevier.com/locate/ejrad

Research article

Quantification of steatosis in alcoholic and nonalcoholic fatty liver disease: Evaluation of four MR techniques versus biopsy

Claire Boudinaud[a,*,1], Armand Abergel[b], Juliette Joubert-Zakeyh[c], Mikael Fontarensky[a], Bruno Pereira[d], Benoit Chauveau[e], Jean Marc Garcier[e], Pascal Chabrot[a], Louis Boyer[a], Benoît Magnin[e]

[a] CHU Gabriel Montpied, Service de radiologie, Clermont-Ferrand, France
[b] CHU Estaing, Service de pathologie digestive et hépato-biliaire, Clermont-Ferrand, France
[c] CHU Estaing, Service d'anatomo-pathologie, Clermont-Ferrand, France
[d] CHU Clermont-Ferrand, DRCI, Unité de Biostatistiques, Clermont-Ferrand, France
[e] CHU Estaing, Service de radiologie, Clermont-Ferrand, France

ARTICLE INFO

Keywords:
Fatty liver
Magnetic resonance imaging
Spectrum analysis
Histological techniques

ABSTRACT

Purpose: Given the growing prevalence of obesity and metabolic syndrome, the management of hepatic steatosis, especially its quantification, is a major issue. We assessed the quantification of liver steatosis using four different MR methods, in order to determine the one that is best correlated with the reference method which consists of histological measurement by liver biopsy.

Method: Seventy-one successive patients requiring liver biopsy for acute or chronic liver disease were enrolled prospectively between March 2017 and March 2018, 11 were excluded and 60 were reported. Liver MR (1.5 T) was organised in order to be performed the same day, using four different steatosis quantification techniques (3-echo MRI, 6-echo MRI, 11-echo MRI and MR Spectroscopy). Quantitative histological and imaging data were compared. In a secondary analysis, we studied the possible influence of alcohol drinking, hepatic iron overload, and the presence of liver fibrosis.

Results: All four MR techniques were found to have excellent correlations with the histological measurements: 3-echo MRI ($r = 0.852$, $p < 0.001$), 6-echo MRI ($r = 0.819$, $p < 0.001$), 11-echo MRI ($r = 0.818$, $p < 0.001$) and MR Spectroscopy ($r = 0{,}812$, $p < 0{,}001$). Interestingly, we also found that the presence of alcohol consumption, iron overload and fibrosis did not interfere with measurements, whichever technique was used.

Conclusion: In the evaluation of hepatic steatosis, our study showed very good correlations of all four MR techniques with the histological standard. There was no confounding factor in a representative group of patients with associated liver conditions such as alcohol consumption, fibrosis and iron overload, for each technique. All four MR techniques may be used in daily practice.

1. Introduction

Hepatic steatosis is caused by the accumulation of triglycerides inside the hepatocytes, due to two main causes: Alcoholic Fatty Liver Disease (AFLD) [1], or Non-Alcoholic Fatty Liver Disease (NAFLD). NAFLD is an increasingly common disease, with a worldwide prevalence estimated at 25% [2–4]. It is associated with the growing prevalence of obesity and metabolic syndrome, which have resulted from changes in eating habits over the last two decades [5–7]. Often asymptomatic at the outset, its clinical implications can be dramatic, ranging from simple steatosis to steatohepatitis (non-alcoholic steatohepatitis or NASH), which can evolve into fibrosis and cirrhosis later on, and subsequent complications (hepatic insufficiency and HCC) [8]. It is the most common chronic liver condition, before alcoholic cirrhosis and hepatitis viral C cirrhosis [9], becoming the primary cause for liver transplants [10–12]. The need for reliable, reproducible and repeatable

Abbreviations: 18F-FDG PET/CT, 18fluorodeoxyglucose positron emission tomography with computed tomography; ALAT, alanin aminotransferase; ALP, alkaline phosphatase; ASAT, aspartate amino transferase; GGT, gamma glutamyl transferase; HCC, hepato cellular carcinoma; HDL, high density lipoprotein; LDL, low density lipoprotein; PDFF, proton density fat fraction; ROI, region of interest

* Corresponding author at: Centre Hospitalier Universitaire Gabriel Montpied, 58 Rue Montalembert, 63000, Clermont-Ferrand, France.
E-mail address: claireboudinaud@msn.com (C. Boudinaud).
[1] Present address: Claire Boudinaud, 68 Rue Paul Collomp, 63000 Clermont-Ferrand.

https://doi.org/10.1016/j.ejrad.2019.07.025
Received 12 May 2019; Received in revised form 12 July 2019; Accepted 18 July 2019

quantification for patient follow-up has become urgent. The gold standard for diagnosing NAFLD is hepatic biopsy [13], but this technique has many drawbacks: it is invasive (leading to risks of haemorrhage), expensive, it doesn't allow complete exploration of the liver, and its quantification usually remains semi-quantitative and subjective. Finally, its estimation does not mirror the actual quantity of hepatic triglycerides, but the proportion of hepatocytes affected. In this framework, CT-scan and ultrasound fail to provide the necessary precision, although quantitative methods are emerging such as Controlled Attenuation Parameter (CAP) using transient elastography [14–17]. Magnetic Resonance techniques have already proved efficient in quantifying steatosis in recent years [18–20]. Proton MR Spectroscopy (1H-MRS), which uses the difference in frequency between lipids and water, is considered as the non-invasive gold standard. Multi-echo gradient-echo MRI, which is based on the difference in phase between water and lipids, enables satisfactory quantification by minimizing effects due to T1-relaxation by applying a low flip angle and by correcting the T2* effect with different echo times; many different sequences have been developed by constructors. Several studies have shown a good correlation of MRS and MRI with histology [21,22] and between each other [23]. To the best of our knowledge, all similar previous studies excluded patients with alcohol consumption or viral hepatitis. The originality of our study is based on synchronous analysis of four MR techniques versus histology in a population reflecting the daily-practice (alcoholic and nonalcoholic patients).

The objective of this study was to evaluate four MR techniques – MR Imaging 3, 6 and 11 echo and MR Spectroscopy - in the quantification of hepatic steatosis of a population of patients with liver diseases in comparison to the reference method, i.e. histological analysis.

2. Material and methods

This prospective study was validated by our national Committee on Protection to Individuals. The Clinical Trial's registry identifier was NCT03142698. All the patients included signed an informed consent form. The employees of Siemens had no rights over the data collected. There was no conflict of interest.

2.1. Study design and patients

A single center, prospective study was carried out between March 2017 and March 2018, based on patients in whom a liver biopsy was required. This population was contacted by the Digestive Diseases Department of the University Hospital of Clermont-Ferrand. The indication for biopsy was determined by a hepatologist. MR examination was performed on the same day as the biopsy or in the days prior to it if necessary. The eligibility criteria were patients requiring a liver biopsy, aged between 18 and 90 years old and who signed informed consent. The inclusions were made without distinction of their underlying liver disease and particularly alcohol consumption wasn't an exclusion criterion. The physician prescribing the examination informed the patients of the study. The exclusion criteria were contraindications to MRI and non-contributory biopsy or MRI.

2.2. Methods

2.2.1. Clinico-biological data

The Body Mass Index (BMI) was calculated in kg/m^2, as defined by the World Health Organisation. We also collected histories of diabetes, dyslipidaemia, current alcohol consumption (> 20 g of alcohol per day for women, > 30 g per day for men), chronic viral B or C hepatitis and cirrhosis. The following biochemical tests were obtained on the same day as biopsy and/or MRI: ASAT, ALAT, GGT, ALP, bilirubin, glucose, triglycerides, HDL and LDL cholesterol.

2.2.2. Biopsy and histological analysis

A transparietal biopsy within the right liver lobe was performed when possible, or in case of contraindications (abnormal coagulation, significant peritoneal effusion) via transjugular liver biopsy. The samples were analysed by a single liver-pathologist (J.JZ) with 20 years' experience, blinded to the MRI results. The proportion of fat was first estimated quantitatively in percentage then classified according to the NASH Clinical Research Network NAFLD activity score and fibrosis score [24], into 4 grades: grade 0, steatosis < 5%, grade 1; steatosis between 5 and 33%; grade 2, steatosis between 33 and 66% and grade 3 steatosis > 66%. Lobular inflammation was graded and fibrosis was evaluated according to the METAVIR score: F0, F1, F2, F3 and F4. Iron overload was evaluated as absent, low, moderate or considerable.

2.3. Radiological analysis (MRI-MRS)

2.3.1. Image acquisition

The examinations were performed on a 1.5-Tesla MRI (Aera, Siemens Healthcare), using a eighteen-channels phased-array body coil, without post-processing filters. An initial axial T2 HASTE morphological sequence was performed at the beginning of each examination. After avoiding T1 effect by applying a low flip angle of 5°, three multi-echo gradient-echo sequences were performed: a 3-echo MR Imaging sequence, consisting of a 2D three-echo gradient-echo sequence lasting 44 s, with the 1st TE at 2.46 ms in phase, the 2nd at 3.69 ms out-of-phase and the 3rd at 4.92 ms in phase; acquisition was volumetric [25]; an 11-echo MR Imaging sequence consisting of a 2D eleven-echo gradient-echo sequence lasting 16 s, with eleven TE every 2.4 ms ranging from 2.4 to 26.4 ms, TR = 120 ms; acquisition was single section passing through the liver and the spleen [26]; and a 6-echo MR Imaging sequence consisting of a Siemens® Liverlab T1 Vibe six-echo gradient-echo sequence, lasting 38 s, with TE = 2.38, 4.76, 7.15, 9.53, 11.91, 14.29 ms; acquisition was volumetric with the positioning of a single ROI at segments V-VI. Then, a MR Spectroscopy sequence was performed, consisting of a single voxel spectroscopy STEAM (Stimulated Echo Acquisition Mode) sequence with a voxel of 3 × 3 x 3 cm, lasting 15 s with TR = 3000 ms, 5 TE at 12, 24, 36, 48, 72 ms for moderate iron concentrations, and at 12, 15, 18, 21, 24 ms for high concentrations, with the positioning of VOI during acquisition at segments V-VI, as for the latter technique.

2.3.2. Post-processing of images

was performed on a SIEMENS® Syngovia console via the MacKesson PACS system, allowing the radiologists (C.B., 4 years of experience and B.M., 8 years of experience), blind to clinico-biological data and to the histological results, to collect the 4 percentages of hepatic fat for each patient; the ROI was placed in the same liver region ((segment V – VI) for each patient and each technique. For the 3-echo MRI sequence, fast calculations of less than two minutes were needed to the operator at the console to obtain a map of the hepatic lipid distribution over the whole volume of the liver. Thus, the percentage of intra-hepatic fat was obtained directly with an ROI of about 1 cm in diameter at segments V-VI. The 11-echo MRI sequence was processed by *Iron By MR* (now called *MRQuantif* in the new version of the website), a post-processing software openly accessible on the web; it consisted in positioning three ROIs in the liver, two ROIs in the para-vertebral muscles, one ROI in the spleen and one ROI in the background noise on a single image, synchronised on the other images corresponding to other TEs. This enabled us to obtain the results of the amount of intra-hepatic fat, intra-hepatic and intra-splenic iron [26]; we considered an iron overload for concentrations > 50 µmol/g. The 6-echo MRI sequence was treated with the LiverLab software, allowing the automatic contouring of the liver and the positioning during acquisition of a ROI inside segments V-VI; this led to the automatic generation of, among others, a diagram showing the percentage of fat and its standard deviation. Finally, again using the Liverlab software for the MRS sequence, spectra and report

were automatically generated containing, among others, the percentage of fat for the VOI positioned during acquisition in the segments V-VI.

2.4. Statistical analysis

The sample size estimation was calculated to highlight a correlation coefficient (between the histological percentage reference and the four percentages obtained by MRI and MRS) greater than 0.50 for a two-sided type I error at 0.001 (correction due to multiple comparisons) and a statistical power greater than 80%. Statistical analyses were performed using Stata software (version 13, StataCorp, College Station, TX, US). Continuous data were expressed as mean ± standard-deviation (SD) or median [interquartile range] according to statistical distribution (assumption of normality assessed using the Shapiro-Wilk test). The study of relationships between quantitative variables was performed using correlation coefficients (Pearson or Spearman, according to the statistical distribution) applying Sidak's correction to take into account the multiples comparisons. Then, a ROC curve analysis was performed to determine the most discriminative approach in relation to the histological results, comparing the ROC curves using DeLong et al method [27]. Furthermore, linear regressions were conducted to estimate conversion coefficients between each MR percentage and the histological percentage. The normality of residuals was studied using the Shapiro-Wilk test. When appropriate, a transformation (logarithmic) was applied to achieve the normality. Finally, the comparison between independent groups was performed using the following statistical tests: for quantitative variables, ANOVA or Kruskal-Wallis test if the assumptions of ANOVA were not met (normality and homoscedasticity studied by the Fisher-Snedecor test) and for categorical parameters, Chi2 test or Fisher's exact tests.

3. Results

3.1. Population (Fig. 1)

During the study period, 71 consecutive patients requiring a liver biopsy were enrolled. 11 were excluded: 3 because of claustrophobia, 2 were fitted with a pace-maker, 4 because of biopsies finally not performed or non-contributive and 2 for non-useable MRI data. Therefore, 60 patients were reported.

3.2. Clinico-biological data (Table 1)

The sixty patients included in our study comprised forty-three men and seventeen women. The average age was 57.9 years. The average BMI was 28.8 kg/m^2; 42% of the patients were obese (25 out of 60).

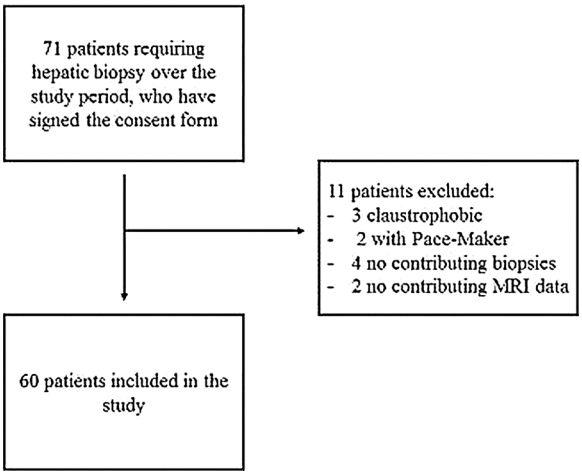

Fig. 1. Flow chart of the study.

Table 1
Demographic, biological, histological and MR Imaging data.

Characteristics of the 60 patients in the study	
Demographic	Total = 60
Age (years)	57.9 ± 12.4 (31-85)
Men, n (%)	43 (72)
Women, n (%)	17 (28)
BMI (kg/m2)	28.8 ± 4.4 (21.5-42)
Cirrhosis, n (%)	35 out of 60 (58)
Regular alcohol consumption, n (%)	23 out of 60 (38)
Diabetes, n (%)	23 out of 60 (38)
Dyslipidemia, n (%)	22 out of 60 (36)
Biopsy	
Transparietal biopsy, n (%)	35 out of 60 (58)
Transjugular biopsy, n (%)	25 out of 60 (42)
Time between MRI and biopsy (days)	0.5 ± 0.3 (0 - 7)
Biology	
AST (U/L)	108 ± 321 (16-2513)
ALAT (U/L)	85 ± 119 (14-750)
GGT (U/L)	238 ± 295 (18-1611)
ALP (U/L)	169 ± 138 (25-815)
Total bilirubin (µmol/L)	72 ± 131 (3-668)
Glycaemia (mmol/L)	5.8 ± 1.5 (2.6-11)
Histology	
Percentage of hepatic steatosis (%)	20.6 ± 20.4 (0-80)
Steatosis Grade 0, n (%)	24 (40)
Steatosis Grades 1, 2, 3, n (%)	36 (60)
Steatosis Grade 1, n (%)	21 (35)
Steatosis Grade 2, n (%)	13 (22)
Steatosis Grade 3, n (%)	2 (3.3)
NASH	17 (28)
Iron overload, n (%)	17 (28)
Fibrosis (Grade ≥ 2), n (%)	39 (65)
Length of biopsy (mm)	20 ± 8 (10 - 45)
Imaging: Proton Density Fat Fraction	
3-echo MRI (%)	5.84% ± 5.3 (0.6 - 22)
11-echo MRI (%)	5.30% ± 5.5 (0.2 - 21.5)
6-echo MRI (%)	5.85% ± 5.0 (0 – 19)
MRSpectroscopy (%)	8.37% ± 6.1 (2 - 25.7)
Iron overload, n (%)	19 (31)

The values are given in numbers over the total number and percentage in parentheses for the discrete quantitative values, and in mean ± standard deviation (minimum – maximum) for the continuous quantitative variables.

Thirty eight percent of the subjects consumed alcohol regularly (23 out of 60), 36% presented dyslipidemia (22 out of 60) and 38% had diabetes (23 out of 60).

3.3. Biopsy (Table 1)

A transparietal biopsy was performed on 58% of the subjects (35 out of 60) and a transjugular biopsy on 42% (25 out of 60). The average length of the biopsy was 20 mm. The biopsy indications were: suspicion of NASH (17 out of 60); assessment of chronic liver disease (11 out of 60) including cirrhosis research in patients with portal hypertension (n = 5), fibrotest-fibroscan discrepancy (n = 3), pre-operative assessment (n = 1), suspected cholangitis (n = 1), suspected sarcoidosis (n = 1); assessment of acute hepatitis (17 out of 60) including alcohol use disorder (n = 16) and unknown aetiology (n = 1); suspected chronic rejection of liver graft (2 out of 60); assessment of non-tumoral liver tissue in patients explored for a nodule (13 out of 60).

Overall, 25 patients had a NAFLD, 16 patients an alcoholic liver disease, 7 a mixed etiology and 12 miscellaneous liver diseases.

3.4. Histological quantification (Table 1)

40% of subjects had grade 0 hepatic lipid overload; 35% of subjects had grade 1; 22% grade 2 and 3% grade 3. Twenty eight percent presented hepatic iron overload, 28% had NASH and 65% had fibrosis grade ≥2. The average percentage of steatosis obtained by histology was 20.6%.

3.5. Quantification in imaging (Table 1)

The average percentage of steatosis detected by imaging was: 5.84% ± 5.3 (range 0.6–22) using the 3-echo MRI technique; 5.30% ± 5.5 (range 0.2–21.5) using the 11-echo MRI technique; 5.85% ± 5.0 (range 0–19) using the 6-echo MRI technique; 8.37% ± 6.1 (range 2–25.7) using the MRS technique.

The average concentration of iron estimated with the 11-echo MRI technique was 40.25 µmol/g.

3.6. Correlation between histology and imaging (Fig. 2)

The four MR techniques provided excellent correlations with the histological measures: the 3-echo MRI technique displayed correlation coefficient $r = 0.852$ ($p < 0.001$), 11-echo MRI: $r = 0.818$ ($p < 0.001$), 6-echo MRI: $r = 0.819$ ($p < 0.001$) and MRS: $r = 0.812$ ($p < 0.001$). The conversion coefficient between the MR percentage and the histological percentage (slope of the correlation plot) was 3.38 for the 3-echo MRI, 3.40 for the 11-echo MRI, 3.17 for the 6-echo MRI and 2.82 for the MRS. ROC-curves are shown in Fig. 3. The areas obtained were 0.97 for the 3 and 6-echo MRI, 0.95 for the MRS and 0.93 for the 11-echo MRI.

The inter-observer agreement was excellent for each technique: 0.98 for the 3-echo MRI, 0.95 for the 11-echo MRI, 1 for the 6-echo MRI and the MRS (because of a single result obtained during the acquisition for these two methods).

3.7. Analysis by subgroups

We evaluated the possible influence of several factors on MR techniques' performance: alcohol consumption, dyslipidemia, diabetes, iron overload, NASH and fibrosis. The results of the histological quantification of steatosis in subgroups as well as the correlation between imaging and histology are presented in Table 2 . It is noteworthy to mention that there is no significant difference in the amount of steatosis according to alcohol consumption, dyslipidemia, diabetes, iron overload or NASH. The amount of steatosis was significantly higher in patients with fibrosis ≥ grade 2 (24.2%) than in patients with grade 0 and 1 fibrosis (13.8%). The estimation of fat proportion remained satisfactory in all subgroups, with no significant difference between patients who regularly consumed alcohol versus those who did not, diabetic or not, dyslipidemic or not, with a fibrosis ≥2 versus those without, with NASH or not and patients with iron overload versus those without.

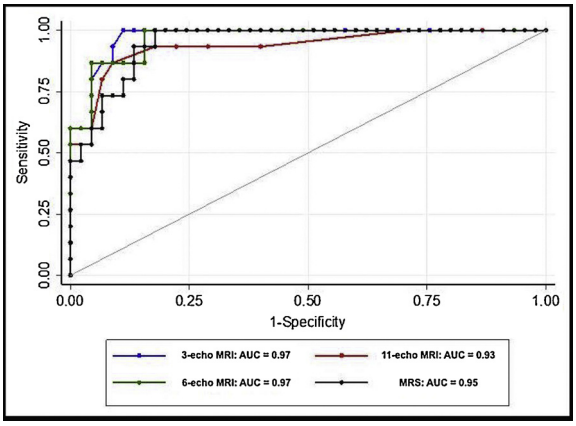

Fig. 3. ROC curves for each MRI technique versus histology.

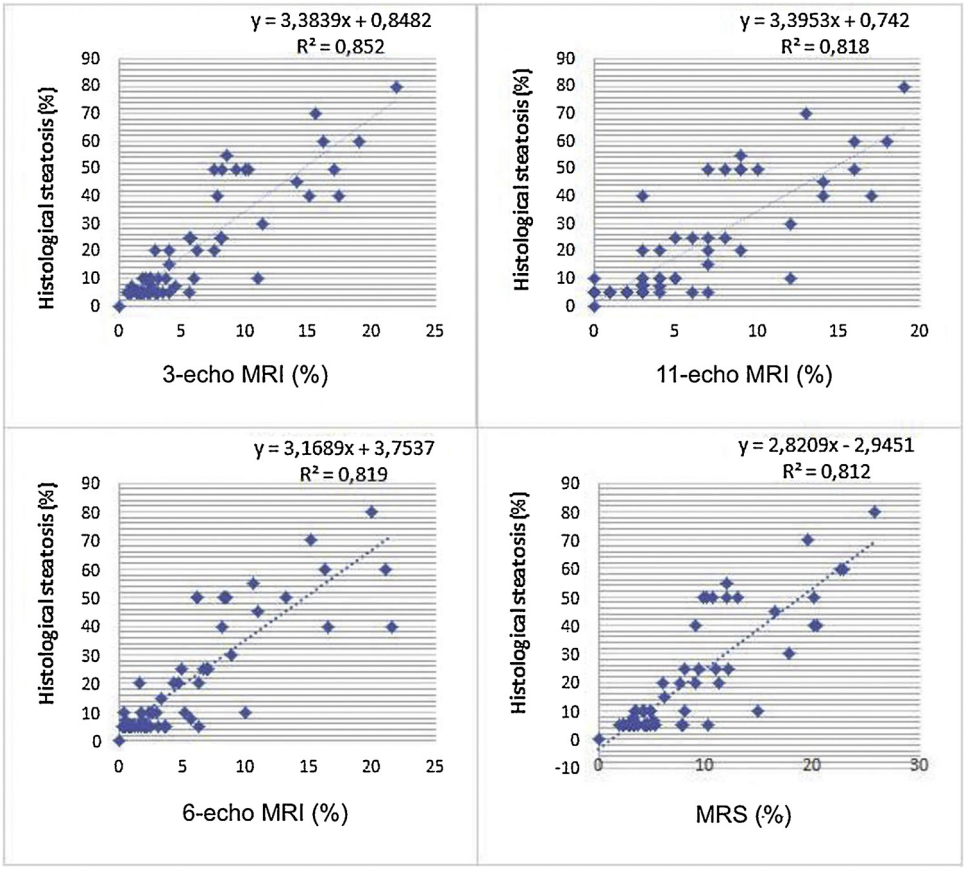

Fig. 2. Correlation curves for each MRI technique in comparison to the histological results.

Table 2
Analysis by subgroups according to different factors: alcohol, diabetes, dyslipidemia, NASH, iron overload, fibrosis.

Parameters	Average percentage of steatosis obtained by histology*	p-value (between the two steatosis percentages)	Correlation coefficient between imaging and histological quantification (r)			
			MRI 3echo	MRI 11echo	MRI 6echo	MRS
Alcohol						
Yes (n = 23)	20.9% ± 19.0	p = 0.74	0.93	0.88	0.89	0.86
No (n = 37)	20.5% ± 21.5		0.84	0.81	0.79	0.84
Diabetes						
Yes (n = 23)	21.4% ± 22.6	p = 0.94	0.87	0.87	0.84	0.84
No (n = 37)	20.1% ± 19.3		0.83	0.78	0.81	0.79
Dyslipidemia						
Yes (n = 22)	25.3% ± 21.7	p = 0.09	0.86	0.87	0.87	0.89
No (n = 38)	17.9% ± 19.4		0.81	0.74	0.75	0.72
NASH						
Yes (n = 17)	24.5% ± 22.4	p = 0.16	0.89	0.90	0.85	0.86
No (n = 43)	19.1% ± 19.7		0.82	0.78	0.77	0.78
Iron overload						
Yes (n = 17)	21.3% ± 19.6	p = 0.73	0.83	0.81	0.76	0.79
No (n = 43)	20.3% ± 21.0		0.85	0.82	0.84	0.83
Fibrosis						
Yes (n = 39)	24.2% ± 22.5	p = 0.02	0.88	0.88	0.84	0.88
No (n = 21)	13.8% ± 13.8		0.79	0.72	0.80	0.75

* The values are given as mean ± standard deviation.

4. Discussion

We have found an excellent correlation between different MR techniques and histology for the quantification of steatosis, confirming previous studies [28,29]. However, our study allowed the comparison of four different MR techniques within a same cohort, with a population that reflected of the daily-practice, including alcoholic patients.

The 3-echo MRI technique appears to provide the best correlation, without any confounding factor negatively affecting the quality of the measures. In addition, it was simple and quick to apply in practice, providing a map of the entire surface of the liver and thus enabling the analysis of the more or less homogenous distribution of overload in fat. Positioning an ROI directly gave the percentage at the desired location.

The 11-echo MRI technique, initially designed for quantifying hepatic iron, was also a robust technique for measuring the lipid fraction, without any secondary factor affecting the results. In our study, we used a single section crossing the liver and the spleen, saving time and manipulation, though limiting the volume of exploration. It is nonetheless possible to perform several sections to analyse the whole liver. The post-processing software was easy to use, making it possible to obtain an automatic report of the percentage of fat and the hepatic and splenic iron concentration, although it required more handling than the 3-echo MRI.

The 6-echo MRI was slightly less reliable than the first two but remained well correlated. It had the advantage of giving the percentage of steatosis directly for the ROI positioned during acquisition. Furthermore, it had the disadvantage of requiring positioning at the time of examination by the radiographer or the radiologist, leading to a risk of irreversible positioning errors and acquisition of one measure only for the whole volume of the liver. Moreover, the presence of iron slightly modified the reliability of the results, although not significantly.

Eventually, MRS remained also a robust technique, even if it had the least precise correlation. Its advantages and disadvantages were the same as for the 6-echo MRI technique regarding manipulation, and a non-significant decrease in measurement reliability in the case of iron overload.

Our analysis focused on a diverse population with relatively open inclusion criteria that did not exclude other causes of chronic liver disease, in particular regular alcohol consumption, in contrast to all previous studies on hepatic steatosis. This was made possible by the very short time between the MRI and the biopsy, on average less than one day, and thus the absence of possible variation of steatosis between two examinations. The study in subgroups showed that the presence of high regular alcohol consumption, dyslipidemia, hepatic fibrosis or presence of iron overload [30] did not adversely affect measurement reliability, whatever the technique. In other words, MRI remains an excellent technique to quantify steatosis in patients with both alcoholic and nonalcoholic fatty liver disease, and will have to be proven on a larger population. These techniques are all very quick to perform, and therefore easily applicable to allow reliable monitoring of patients over time, such as in a recent study on oncologic patients [31].

A limitation of our study was the low number of patients with high steatosis (grade 3: 3.3%). The number of subjects was estimated for the primary objective; conclusions about secondary analysis, including alcohol consumption, should be confirmed on a larger population.

In conclusion, our study showed that in a daily-pratice population without the exclusion of patients consuming alcohol, any of the MR techniques studied could be used with confidence to quantify liver steatosis, regardless of the underlying liver disease.

Declaration of Competing Interest

None.

References

[1] M. Teli, C. Day, O.F. James, et al., Determinants of progression to cirrhosis or fibrosis in pure alcoholic fatty liver, Lancet 346 (1995) 987–990, https://doi.org/10.1016/S0140-6736(95)91685-7.
[2] J. Maurice, P. Manousou, Non-alcoholic fatty liver disease, Clin Med 18 (2018) 245–250, https://doi.org/10.7861/clinmedicine.18-3-245.
[3] Z.M. Younossi, A.B. Koenig, D. Abdelatif, et al., Global epidemiology of nonalcoholic fatty liver disease-Meta-analytic assessment of prevalence, incidence, and outcomes, Hepatology 64 (2016) 73–84, https://doi.org/10.1002/hep.28431.
[4] S. Bellentani, The epidemiology of non-alcoholic fatty liver disease, Liver Int. 37 (2017) 81–84, https://doi.org/10.1111/liv.13299.
[5] R. Vuppalanchi, N. Chalasani, Nonalcoholic fatty liver disease and nonalcoholic steatohepatitis: selected practical issues in their evaluation and management, Hepatology 49 (2009) 306–317, https://doi.org/10.1002/hep.22603.
[6] P. Angulo, Nonalcoholic fatty liver disease, J. Gastroenterol. Hepatol. (2002).
[7] T.J. Fraum, D.R. Ludwig, S. Kilian, et al., Epidemiology of hepatic steatosis at a tertiary care center, Acad. Radiol. 25 (2018) 317–327, https://doi.org/10.1016/j.acra.2017.10.002.
[8] C. Matteoni, Z. Younossi, T. Gramlich, et al., Nonalcoholic fatty liver disease: a spectrum of clinical and pathological severity, Gastroenterology 116 (1999) 1413–1419, https://doi.org/10.1016/S0016-5085(99)70506-8.
[9] L.A. Adams, K.D. Lindor, Nonalcoholic fatty liver disease, Ann. Epidemiol. 17 (2007) 863–869, https://doi.org/10.1016/j.annepidem.2007.05.013.
[10] M.R. Charlton, J.M. Burns, R.A. Pedersen, et al., Frequency and outcomes of liver

transplantation for nonalcoholic steatohepatitis in the United States, Gastroenterology 141 (2011) 1249–1253, https://doi.org/10.1053/j.gastro.2011.06.061.
[11] R.J. Wong, M. Aguilar, R. Cheung, et al., Nonalcoholic steatohepatitis is the second leading etiology of liver disease among adults awaiting liver transplantation in the United States, Gastroenterology 148 (2015) 547–555, https://doi.org/10.1053/j.gastro.2014.11.039.
[12] C.D. Byrne, G. Targher, NAFLD: a multisystem disease, J. Hepatol. 62 (2015) S47–S64, https://doi.org/10.1016/j.jhep.2014.12.012.
[13] P. Bedossa, Pathology of non-alcoholic fatty liver disease, Liver Int. 37 (2017) 85–89, https://doi.org/10.1111/liv.13301.
[14] J.-Y. Son, J.Y. Lee, N.-J. Yi, et al., Hepatic steatosis: assessment with acoustic structure quantification of US imaging, Radiology 278 (2016) 257–264, https://doi.org/10.1148/radiol.2015141779.
[15] J.H. Runge, L.P. Smits, J. Verheij, et al., MR spectroscopy–derived proton density fat fraction is superior to controlled attenuation parameter for detecting and grading hepatic steatosis, Radiology 286 (2018) 547–556, https://doi.org/10.1148/radiol.2017162931.
[16] K. Shimizu, T. Namimoto, M. Nakagawa, et al., Hepatic fat quantification using automated six-point Dixon: comparison with conventional chemical shift based sequences and computed tomography, Clin. Imaging 45 (2017) 111–117, https://doi.org/10.1016/j.clinimag.2017.06.006.
[17] V. Bhat, Quantification of liver fat with mDIXON magnetic resonance imaging, comparison with the computed tomography and the biopsy, J. Clin. Diagn. Res. 2017 (11) (2017) TC06–TC10, https://doi.org/10.7860/JCDR/2017/26317.10234.
[18] F.H. Cassidy, T. Yokoo, L. Aganovic, et al., Fatty liver disease: MR imaging techniques for the detection and quantification of liver steatosis, RadioGraphics 29 (2009) 231–260, https://doi.org/10.1148/rg.291075123.
[19] M. Koplay, Importance of imaging and recent developments in diagnosis of nonalcoholic fatty liver disease, World J. Hepatology 7 (2015) 769, https://doi.org/10.4254/wjh.v7.i5.769.
[20] H. Hetterich, C. Bayerl, A. Peters, et al., Feasibility of a three-step magnetic resonance imaging approach for the assessment of hepatic steatosis in an asymptomatic study population, Eur. Radiol. 26 (2016) 1895–1904, https://doi.org/10.1007/s00330-015-3966-y.
[21] I.S. Idilman, A. Tuzun, B. Savas, et al., Quantification of liver, pancreas, kidney, and vertebral body MRI-PDFF in non-alcoholic fatty liver disease, Abdom. Imaging 40 (2015) 1512–1519, https://doi.org/10.1007/s00261-015-0385-0.
[22] I.S. Idilman, H. Aniktar, R. Idilman, et al., Hepatic steatosis: quantification by proton density fat fraction with MR imaging versus liver biopsy, Radiology 267 (2013) 767–775, https://doi.org/10.1148/radiol.13121360.
[23] T. Yokoo, S.D. Serai, A. Pirasteh, et al., Linearity, Bias, and precision of hepatic proton density fat fraction measurements by using MR imaging: a meta-analysis, Radiology 286 (2018) 486–498, https://doi.org/10.1148/radiol.2017170550.
[24] D.E. Kleiner, E.M. Brunt, M. Van Natta, et al., Design and validation of a histological scoring system for nonalcoholic fatty liver disease, Hepatology 41 (2005) 1313–1321, https://doi.org/10.1002/hep.20701.
[25] B. Guiu, J.M. Petit, R. Loffroy, et al., Quantification of liver fat content: comparison of triple-echo chemical shift gradient-echo imaging and in vivo proton MR spectroscopy, Radiology 250 (1) (2009) 95–102, https://doi.org/10.1148/radiol.2493080217.
[26] Principle of joint quantification of iron and liver fat by MRI. https://imagemed.univ-rennes1.fr/fr/mrquantif/quantif.php, (Accessed 27 Jun 2018).
[27] E.R.1 DeLong, D.M. DeLong, D.L. Clarke-Pearson, Comparing the areas under two or more correlated receiver operating characteristic curves: a nonparametric approach, Biometrics. Sep 44 (3) (1988) 837–845.
[28] X. Wang, X. Zhang, L. Ma, Diagnostic performance of magnetic resonance technology in detecting steatosis or fibrosis in patients with nonalcoholic fatty liver disease: a meta-analysis, Medicine 97 (2018) e10605, , https://doi.org/10.1097/MD.0000000000010605.
[29] M.S. Middleton, E.R. Heba, C.A. Hooker, et al., Agreement between magnetic resonance imaging proton density fat fraction measurements and pathologist-assigned steatosis grades of liver biopsies from adults with nonalcoholic steatohepatitis, Gastroenterology 153 (2017) 753–761, https://doi.org/10.1053/j.gastro.2017.06.005.
[30] D.E. Horng, D. Hernando, S.B. Reeder, Quantification of liver fat in the presence of iron overload: liver Fat in Iron overload, J. Magn. Reson. Imaging 45 (2017) 428–439, https://doi.org/10.1002/jmri.25382.
[31] G. Corrias, S. Krebs, S. Eskreis-Winkler, et al., MRI liver fat quantification in an oncologic population: the added value of complex chemical shift-encoded MRI, Clin. Imaging 52 (2018) 193–199, https://doi.org/10.1016/j.clinimag.2018.08.002.